Talanta 85 (2011) 2504–2510

Contents lists available at ScienceDirect

Talanta

journal homepage: www.elsevier.com/locate/talanta

Investigation of uranium–colloid interactions in soil by dual field-flow fractionation/capillary electrophoresis hyphenated with inductively coupled plasma-mass spectrometry

Céline Claveranne-Lamolère[a,b], Jean Aupiais[b], Gaëtane Lespes[a], Jérôme Frayret[a], Eric Pili[b], Fabien Pointurier[b], Martine Potin-Gautier[a,*]

[a] Université de Pau et des Pays de l'Adour, CNRS-LCABIE, UMR 5254 IPREM, 2 avenue P. Angot, 64000 Pau, France
[b] CEA-DAM, DIF F-91297 Arpajon, France

ARTICLE INFO

Article history:
Received 5 April 2011
Received in revised form 26 July 2011
Accepted 29 July 2011
Available online 5 August 2011

Keywords:
Flow field-flow fractionation
Capillary electrophoresis
ICP-MS
Colloids
Uranium

ABSTRACT

This paper deals with the study of uranium–colloid interactions in a carbonated soil. The work is focused on the immediately available fraction obtained after a leaching process, according to a normalized batch method. In order to characterize the different colloidal carriers, Asymmetrical Flow Field-Flow Fractionation (As-Fl-FFF) coupled to different detectors (UV, Multi Angle Laser Light Scattering (MALLS) and Inductively coupled Plasma-Mass Spectrometry (ICP-MS)) was used. The colloidal carriers are mainly inorganic particles (carbonated particles and clays) mixed with organic substances. Furthermore, dissolved and colloidal uranium species in the leaching solutions were monitored by Capillary Electrophoresis (CE) coupled to ICP-MS, in order to investigate the uranium/colloids interactions. According to the first results, uranium fate in this specific soil is controlled by sorption/desorption phenomena, strongly pH dependent.

1. Introduction

Uranium is an actinide naturally present in the environment. It has three naturally occurring isotopes: ^{238}U (natural abundance 99.275%), ^{235}U (0.720%) and ^{234}U (0.005%) [1]. It is mainly used as fuel for the reactors of nuclear power plants (uranium enriched in ^{235}U). Other applications are armor plating or anti-tanks shells (depleted uranium). Today, with new needs like nuclear site monitoring, storage in deep geologic environment, accidental pollutions or simulations, it is of utmost importance to estimate the mobility of uranium in the different environmental compartments, in order to predict its long-term behavior.

The International Union of Pure and Applied Chemistry (IUPAC) defines the term colloidal as corresponding to "a state of subdivision implying that molecules or polymolecular particles dispersed in a medium have, at least in one direction, a dimension between 1 nm and 1 μm" [2]. According to this definition, in soil, colloids comprise a wide range of entities: iron or aluminium hydroxides, manganese oxides, clays, carbonates, organic matter (humic substances), polysaccharides, virus, bacteria, etc. [3]. Over the last decade, many studies brought to light the key role of colloids in trace metal transport. In view of their high surface area and strong chelating capacity, colloids have been implicated in the transport of many elements including uranium [4,5]. Several recent studies of actinide–colloid interactions have been done [6–13]. However, the results of these studies vary widely; for example, colloids can either increase or decrease the mobility and the percentage of actinide transported by colloids ranges from 0 to 100%. Finally, conditions and mechanisms of transport are unknown or differ greatly. These differences can generally be explained by the great variability of the studied sites, various physico-chemical conditions observed and different types of colloids present. Moreover, many questions remain unsolved for instance what is the speciation of the actinide associated to colloids, what is the size and the nature of carriers and finally what kind of mechanisms drive these interactions [14].

Due to of the complexity of environmental colloids and because the use of a single analytical technique provides only a limited amount of information, a multi-technique analytical approach is generally required [15–19]. Due to their polydispersity, size-fractionation of environmental colloids is generally the first step. Flow Field-Flow Fractionation (Fl-FFF) has taken an important place among the different separative tools because of its high resolution, its capability to fractionate over a wide range of size and the lower interactions with the analytical system. Moreover, it can be easily coupled to various detectors like Ultra-Violet (UV),

Abbreviations: As-Fl-FFF, Asymmetrical Flow Field-Flow Fractionation; MALLS, Multi Angle Laser Light Scattering; ICP-MS, Inductively Plasma-Mass Spectrometry; CE, Capillary Electrophoresis.

* Corresponding author. Tel.: +33 5 59 40 76 69; fax: +33 5 59 40 76 74.
E-mail address: martine.potin@univ-pau.fr (M. Potin-Gautier).

0039-9140/$ – see front matter © 2011 Elsevier B.V. All rights reserved.
doi:10.1016/j.talanta.2011.07.100

Multi Angle Laser Light Scattering (MALLS), Fluorescence, Differential Refractive Index (RI) or Atomic Spectrometer. Such couplings give data as molar masses, hydrodynamic or gyration radius, element composition, etc. [20,21]. Asymmetrical Fl-FFF (As-Fl-FFF) is a sub-technique of Fl-FFF where the cross-flow is generated by a differential pressure in a semi-permeable channel. The As-Fl-FFF system is also easy to use, the superior wall in plexiglas enables observation of the elution and this technique allows the fractionation speed to be increased and involves less dilution [20].

Capillary Electrophoresis (CE) has also been recognized as an efficient tool in the nanotechnologies studies [22]. Its advantages include high power of resolution, speed of analysis and small sample size (nL) [23]. In addition, it can be coupled to a lot of detectors. The most used are absorption spectroscopies, typically UV including fixed wavelength or diode array detector (PDA) [24–26], Inductively Coupled Plasma-Mass Spectrometry (ICP-MS) [23–27] and Laser-Induced Fluorescence (LIF) [28]. Although CE-ICP-MS coupling is efficient for trace metal analysis, it is also difficult to be operated. Indeed, numerous conditions linked to the characteristics of both techniques have to be considered. The most important are the adaptation of the flow rate in the outlet of the electrophoresis (0.1 $\mu L\,min^{-1}$) to the inlet of the detector (1–1000 $\mu L\,min^{-1}$) and the lock of the CE electric circuit [29]. To achieve these conditions, a specific interface is required. Despite these constraints, this coupling remains a tool of choice in bioenvironmental studies because of the high CE separation power, ICP-MS sensitivity and capability of elemental multi-detection.

The aim of this work was to investigate uranium–colloid interactions using As-Fl-FFF-multi-detection and CE-ICP-MS coupling. To achieve the colloidal characterization, As-Fl-FFF-multi-detection (UV, MALLS and ICP-MS) was used. Then by considering different pH, the variation of affinity between uranium and colloid surface sites was studied by CE-ICP-MS. The specific objective was to determine the influence of pH on the colloidal interactions of uranium (colloids $\leq$ 450 nm).

2. Materials and methods

2.1. Chemicals

Acetic acid (CH_3COOH: 99–100%) and ammonium nitrate (NH_4NO_3: 98.5%) were purchased from Baker (Deventer, Holland) respectively in order to prepare CE and FFF mobile phases. Boric acid (99.5%) used during the mineralization step was purchased from Prolabo (Paris, France). N-(2-hydroxyethyl) piperazine-2′-(2-ethanesulfonic acid) (HEPES sodium salt, CE buffer) was obtained from Aldrich (St Louis, USA). Sodium acetate (CE buffer) was purchased from Atlantic Labo (Eysines, France). De-ionized water with a conductivity of 18 MΩ was obtained with a Milli-Q system (Millipore, USA). For sample filtrations before analysis, 0.45 and 0.02 μm cellulose acetate filters were used (Millipore, USA). Hydrodynamic diameter calibration was carried out using Polystyrene Standards (PS) (40, 80, 200, 300, 400, 500 and 600 nm diameter) (Duke Scientific Corporation, Fremont, USA).

2.2. Soil samples and leaching protocole

The soil of interest came from a site ideally located for studying uranium water/rock interactions. It is a site of interest for the CEA. The soil was a rendosol, *i.e.* a thin layer of a brown and organic soil on a carbonated bed-rock (95% $CaCO_3$). Samples were collected from the same location at 0–30 cm depth (*i.e.* brown-organic soil). This soil fraction is known to be rich in humic substances and clays. All samples were collected with shovels and trowels in plastic bags and stored at 4 °C until analysis.

In order to collect the fraction of the soil assumed to be easily mobilizable, batch experiments were performed according to a protocol from the French Agency of Normalization (AFNOR) [30]. Fifty grams of the brown soil was leached with 50 mL of a leaching reagent in a vial shaken for 24 h (liquid/solid ratio (L/S) equal to 1). Artificial rain water was used as leaching agent to simulate the influence of the rain onto surface of the soil. According to Davies et al. [31], the following inorganic salts were added per 1000 L of de-ionized water to obtain the solution: $NaNO_3$, 4.07 g – NaCl, 3.24 g – KCl, 0.35 g – $CaCl_2{\cdot}2H_2O$, 1.65 g – $MgSO_4{\cdot}7H_2O$, 2.98 g and $(NH_4)_2SO_4$, 3.41 g. This composition is typical of those from both Northern and Southern hemispheres [31]. It had an ionic strength of 0.3 mmol L^{-1} and a pH of 5.8. Then, the slurry was centrifuged at 3500 rpm for 30 min. Finally the supernatant was collected and filtered at the desired cut-off (0.45 μm or 0.02 μm – see later on in Section 3.3) before analysis.

2.3. Instruments and procedures

2.3.1. Field-Flow Fractionation

A Flow Field-Flow fractionation system (Eclipse 3, Wyatt Technology, Dernbach, Germany) with an asymmetrical channel was used in this work. The length of the channel was 26.5 cm and its width ranged from 0.6 to 2.1 cm. Its thickness was defined by a spacer according to analytical conditions (see below). FFF ultrafiltration membranes used in the FFF system were 1 kDa (cut-off) polyethersulfone (Postnova, Landsberg, Germany) and 10 kDa regenerated cellulose (Wyatt, Technology, Dernbach, Germany). Flows were controlled with an Agilent 1100 series isocratic pump equipped with an Agilent series micro-vacuum degasser (Agilent Technology, Tokyo, Japan). The HPLC pump used for the quantification was a Varian 9012 (Varian, Palo Alto, USA).

The UV detector was an adjustable wavelength 1100 series (Agilent Technology, Tokyo, Japan) tuned at 254 nm. The MALLS was a Dawn-Heleos II (Wyatt Technology, Santa Barbara, USA). The ICP-MS was an Agilent 7500ce model (Agilent Technology, Tokyo, Japan) with a Meinhard nebulizer.

The run sequences contained first two short (2 min) and consecutive steps of elution and focused without injection to equilibrate the system and follow the baseline. Then, the injection started with a focus (5 min). This step allows keeping colloids at head of the channel. After the sample injection, the focus step was then kept for 6 min to reduce the lateral extension of the sample due to the injection. Finally, the elution started with cross-flow, leading to colloidal fractionation. When the fractionation step was over, a rinse step without cross-flow was applied (5 min).

Concerning the hyphenation of As-Fl-FFF and ICP-MS, the output of the last detector (MALLS) was directly connected to the nebulizer of the ICP-MS via a capillary tube allowing the As-Fl-FFF effluent to be introduced into the ICP-MS system. The different isotopes monitored were ^{56}Fe, ^{27}Al, ^{44}Ca, ^{24}Mg, ^{48}Ti and ^{238}U. The collision cell with H_2 as collision gas was used to decrease interferences especially ^{56}Fe (interfered by $^{40}Ar^{16}O$) and ^{44}Ca (interfered by $^{12}C^{16}O_2$) (gas rate: 4 mL min^{-1}).

In order to have an efficient fractionation power (from 1 to 450 nm), the fractionation was performed by using the analytical conditions previously optimized and described [32]. The fractionation in Fl-FFF normal mode is controlled by the diffusion coefficient of the analytes. The hydrodynamic diameter is linked to the retention parameter (R) according to Eq. (1) [33]:

$$D_h = \frac{2ktV_0}{\pi\eta V_c w^2}\frac{(1-R)^{1/3}}{R} \quad (1)$$

where V_0 is the void volume (m^3), V_c is the cross-flow ($m^3\,s^{-1}$), η is the viscosity of the mobile phase ($kg\,m^{-1}\,s^{-1}$), R is the retention

parameter defined as t_0/t_R (ratio between void time and retention time), w is the channel thickness (m) and k is the Boltzmann constant ($k = 1.38 \times 10^{-23}$ kg m^2 s^{-2} K^{-1}).

At constant operating conditions and when t_R is sufficiently high (meaning $t_0/t_R \ll 1$), the formula (1) can be simplified in a linear relationship between D_h and t_R:

$$D_h = At_R \quad (2)$$

with A, a constant including parameters of (1).

2.4. Capillary electrophoresis

A commercial Beckman Coulter P/ACE MDQ CE system (Beckman Coulter, Fullerton, USA) equipped with a UV detection mode was used for all separations. It was provided with a tailor-made capillary cartridge support designed for the use of an external detector. A conventional fused silica column of 75 μm internal diameter capillary (Bechkman Coulter, Fullerton, USA) and 65 cm length was used for separations. An optical window was placed at 10.2 cm (l) from the capillary inlet. The capillary was maintained at a constant temperature of 25 °C thanks to a coolant wrapped around the capillary. The capillary outlet was placed 1 mm back from the nebulizer tip to ensure the electrical continuity of the circuit [34].

An Agilent 7500ce ICP-MS (Agilent Technology, Tokyo, Japan) was coupled with the CE device for the detection of uranium and major ions species (see results and discussion). A commercial parallel-path micro-nebulizer (Mira Mist CE, Burgener, Ontario, Canada) was used with a make-up solution (2% HNO_3/10% ethanol). This make-up liquid was introduced using a syringe pump 11 Pico Plus (Harvard Apparatus, Holliston, USA) to maintain a nominal flow rate of 9 μL min^{-1}.

Before each separation, the capillary was washed with the electrolyte for 5 min at 20 psi. Sample injections were carried out hydrodynamically at 5 s, 3 psi. Separations were achieved at a constant voltage of 15 kV. They were completed within 20 min.

In order to reliably sweep a large pH range, seven buffer solutions as background electrolytes were used: potassium hydrogen phthalate (pH 3 and 4), ammonium acetate (pH 5), ammonium nitrate (pH 6), HEPES (pH 7) and Tris(hydroxymethylaminomethane) hydrochloride (Tris) (pH 8) *i.e.* a solution of Tris adjusted to pH 8 by the addition of HCl. Concentrations were adjusted such that the ionic strength of the solution is 10^{-3} mol L^{-1}.

The monitoring of uranium and major ions was performed by ICP-MS. It was realized according to the same optimized conditions used in As-Fl-FFF (see Section 2.3.1.). Contrary to FFF, the hyphenation between CE and ICP-MS allowed to monitor dissolved and colloidal species according to the cut-off of the different filters used before analysis.

In capillary electrophoresis, the velocity of an ion i (ν_i in m s^{-1}) is calculated by the Eq. (3):

$$\nu_i = \mu_{ep} \times E \quad (3)$$

where μ_{ep_i} (m^2 s^{-1} V^{-1}) is the electrophoretic mobility of i and E (V m^{-1}) the electric field applied between the capillary inlet and outlet.

From the CE-ICP-MS analysis, the apparent mobility μ_{app_i} is the sum of μ_{ep} and μ_{eof} (μ_{ep}, the electrophoretic mobility and μ_{eof}, the electroosmotic mobility). It was experimentally determined thanks to the Eq. (4):

$$\mu_{app} = \frac{Ll}{V} \times \left(\frac{1}{t_i} - \frac{1}{t_{eof}}\right) \quad (4)$$

where L (cm) is the total length of the capillary, l (cm) the length up to the location of the window, t_i (s) the migration time of a species i between the injection and the ICP-MS detection and t_{eof} (s) the migration time of a neutral species (N,N-dimethylformamide (DMF) in this study) allowing to determine the electroosmotic flow. t_{eof} is measured and brought back in L to be coherent with regard to t_i.

2.5. Species predictions

To determine uranium chemical species which could be present under the conditions of this study, without considering colloidal ligands, speciation calculations were performed thanks to the "Species" software from the Academic software (Timble, Otley, United Kingdom) available in the laboratory. Thermodynamic constants recommended by the Nuclear Energy Agency (NEA) and the Organisation for Economic Co-operation and Development (OECD) presented in Table 1 were used.

The uranium concentration was set at 10^{-8} mol L^{-1}, according to a previous study allowing the uranium quantification in the same samples [32]. The carbonated species concentrations were defined thanks to the dissolution of carbon dioxide in the leaching reagent. So, constants were recalculated for an ionic strength ranges from 10^{-3} to 10^{-1} mol L^{-1}. Indeed, despite the fact that experiments were performed at 10^{-3} mol L^{-1}, the pH variation from acidic to alkaline conditions leads to an increase of the carbonate concentration since all solutions tend to equilibrate with air. The distribution of the species obtained for 10^{-1} mol L^{-1} must be also considered as the limiting distribution.

3. Results and discussion

3.1. Characterization of the colloidal carriers

In the first step of this study, colloidal carriers present in soil leachates were characterized in size and chemical composition by As-Fl-FFF-ICP-MS coupling. Typical size distributions (hydrodynamic diameter) of the colloids present in the soil leachate obtained (*A-MALLS and UV signals*) and the major elements observed (*from B to G*) are given in Fig. 1. These major elements have been observed in a previous work [32]. Complementary, gyration diameters (calculations made by Astra software) are also mentioned in Fig. 1A.

In leachates, the colloidal population appears to be polydisperse (strong MALLS signal and non Gaussian profile). It could

Table 1
Values of the different parameters injected for the speciation calculations, the stability constants have been corrected for $I = 10^{-3}$ mol L^{-1} and $I = 10^{-1}$ mol L^{-1} by Davies theory.

Initial ions	Concentration (10^3 mol L^{-1})	
UO_2^{2+}	0.00001	
CO_3^{2-}	75.28	
Predicted species	**log β (10^{-3} mol L^{-1})**	**log β (10^{-1} mol L^{-1})**
OH^-	−14	−14
UO_2OH^+	−5.28	−6.1
$UO_2(OH)_2$	−12.18	−13.38
$UO_2(OH)_3^-$	−20.28	−21.48
$UO_2(OH)_4^{2-}$	−32.43	−33.16
$(UO_2)_2OH^-$	−2.73	−2.7
$(UO_2)_2(OH)_2^-$	−5.65	−6.87
$(UO_2)_3(OH)_4^{2+}$	−11.93	−14.38
$(UO_2)_3(OH)_5^+$	−15.58	−16.46
$(UO_2)_3(OH)_7^-$	−32.23	−33.39
$(UO_2)_4(OH)_7^-$	−21.93	−22.23
UO_2CO_3	9.82	9.08
$UO_2(CO_3)^{2-}$	16.49	15.76
$UO_2(CO_3)_3^{4-}$	21.84	21.89
HCO_3^-	10.27	9.9
H_2CO_3	16.68	16.05
$(UO_2)_2CO_3(OH)_3^-$	−19.04	−19.75

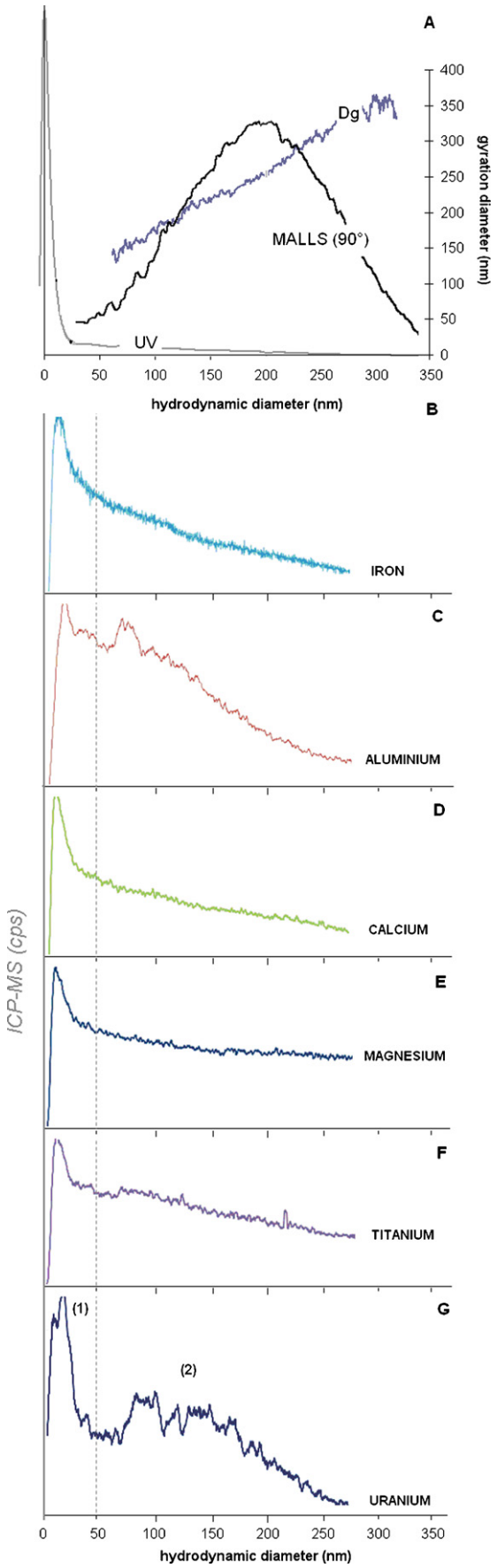

Fig. 1. Typical size distribution of colloids obtained from the soil leachate.

seem to be inorganic since there is no UV response. The hydrodynamic diameters (D_h) go up to 300 nm and the gyration diameters (D_g) range from 100 to 350 nm. Iron, aluminium, magnesium, calcium and titanium are the major ions detected in the colloidal phase. Additionally, according to the Total Inorganic Carbon (TIC) measurements, 75% of the total carbon contained in the colloidal fraction was found to be inorganic. From a previous work on the same soil, humic-like substances and inorganic colloidal particles including iron, aluminium and carbonated nanoparticles were mainly detected [32]. In the present study, the presence of carbonated particles was also expected as the soil is on a carbonated bed-rock. So, the colloidal population was assumed to be constituted by aggregates of inorganic and organic entities, such as carbonated particles (more generally carbon-based particles), inorganic particles containing iron and aluminium (for example oxyhydroxydes) and organic matter (humic-like substances or polysaccharides according to diameters).

Considering uranium, its distribution overlaps the MALLS signal, showing that uranium is significantly associated with the whole colloidal population. This distribution appears to be bimodal (indicated by (1) and (2) on Fig. 1G) suggesting that this element could be associated to two types of colloids. The same phenomenon seems to be observed for Al (Fig. 1C).

3.2. Species predictions

Then, in order to determine uranium chemical species which could be present under the conditions of this study, speciation calculations were performed. The results are presented in Fig. 2.

In addition, the average apparent charge of the uranium species in equilibrium was calculated as a function of pH (Fig. 3) according to the formula (5):

$$Q_A = \frac{\sum [\text{ions}]^{zj}}{\sum [\text{species}]} \tag{5}$$

With Q_A, the average apparent charge, zj the charge of the species considered, $[\text{ions}]^{zj}$ the concentration of the charged ions zj and $\sum[\text{species}]$ the total concentration of the species considered.

These both figures were used jointly to comment the results obtained from CE-ICP-MS (see below in the text).

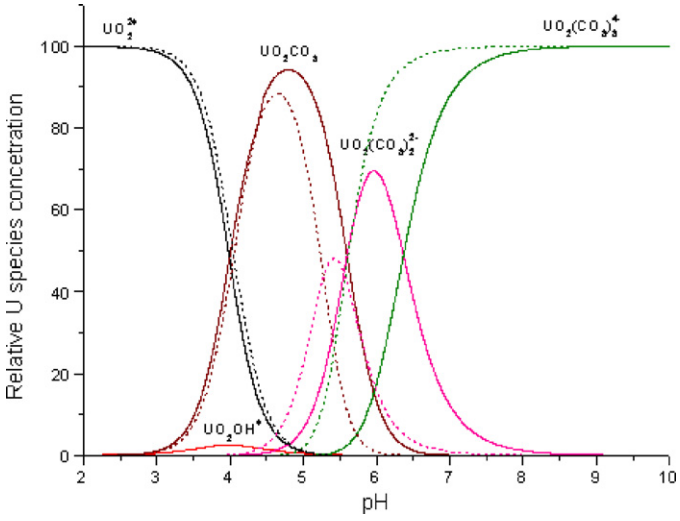

Fig. 2. Speciation diagram of 10^{-8} mol L^{-1} uranium in the 10^{-3} mol L^{-1} (solid lines) and 10^{-1} mol L^{-1} (dashed lines) non-complexing leaching solutions in equilibrium with the atmosphere.

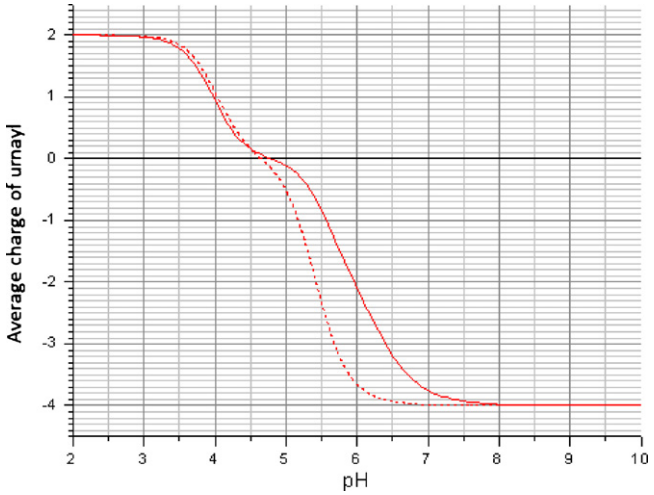

Fig. 3. Average charge of uranyl species for $I = 10^{-3}$ mol L^{-1} (solid line) and 10^{-1} mol L^{-1} (dash line) in equilibrium in function of the pH.

3.3. Uranium species in dissolved and colloidal phases

The last part of this work is dedicated to understand how uranium and colloids interact under the study conditions. To do so, the hyphenation between CE and ICP-MS was used and typical electropherograms of the soil leachate are given in Fig. 4. Major elements were selected according to the first observations made by As-Fl-FFF. By considering different pH (from acidic rain waters to carbonated bed-rock), the variation of affinity between uranium and colloid surface sites were evaluated.

Then, the apparent mobilities of uranium and the major elements experimentally determined (see Fig. 4) for the different pH are presented in Table 2.

Only a broad band is observed on the electropherograms, resulting in fast equilibriums between uranium chemical species. As a result, the location of the uranium peak in the cationic and/or anionic areas of each electropherogram depends on the global average charge of the physico-chemical species with which uranium is associated over dissolved and colloidal phases.

Additionally, it is obviously difficult to conclude on the nature of each peak observed. Indeed this work is based on real samples, initially considered over 0–450 nm (see Section 2) and so containing dissolved and colloidal species. In order to have a narrower range of size, the soil leachate was subsequently, filtered at 0.02 μm before analysis (the smallest cut-off available). This operation led to observe the dissolved part and only colloids smaller than 20 nm. Typical electropherograms are presented in Fig. 5.

Table 2
Apparent mobilities ($\times 10^4$ m^2 V^{-1} s^{-1}) concerning the species observed by CE-ICP-MS. Calculation uncertainties: ($\pm 0.03 \times 10^4$ cm^2 V^{-1} s^{-1}).

Parameters	pH 3	pH 4	pH 5	pH 6	pH 7	pH 8
$^{*}\mu_{eo}$	3.11	6.20	7.97	8.36	7.41	10.23
$^{**}\mu_{app}(U)$	0.64	−1.07	−3.63	−1.86	−2.96	−1.09
$^{**}\mu_{app}(Mg)$	5.31	4.52	3.79 2.88	3.86	3.31	3.42
$^{**}\mu_{app}(Ti)$	4.83	5.30	3.71	4.08	3.36	3.63

$^{*}\mu_{eo}$: electroosmotic mobility, $^{**}\mu_{app}$: apparent mobility.

Only three elements were detected on the different electropherograms (Figs. 4 and 5), *i.e.* magnesium, titanium and uranium. Their electrophoretic mobility values cannot be compared from one pH to the others because of media differences of the electrolytic solutions. However, these mobilities allow specifying two things: on one hand the elements that can be assumed to be present in a same physico-chemical species for the same pH and, on the other hand, the cationic or anionic nature of these species, given that uranium can be under molecular or ionic dissolved forms, as well as associated with colloidal carriers. The observed peaks mainly are broad, reminding polydisperse populations. Mg and Ti having been previously identified as constituents of colloids, this observation supports also the hypothesis of colloidal populations observed here. Thanks to the comparison between both sets of electropherograms (Figs. 4 and 5), obtained in the same separation media, it is possible to determine which species belongs to the colloidal (>20 nm) and/or to the "dissolved" phase (strictly dissolved phase and colloidal phase <20 nm). These observations, jointly used with the speciation information and the colloidal characterization, lead to propose uranium speciation and distribution over the dissolved-colloidal compartments. The whole information is presented in a greater detail as well as commented later on.

At pH 3, a single uranium peak is observed. It is located in the cationic zone of the electropherogram, showing the cationic nature of the corresponding detected species. No correlation is observed between the electrophoretic mobilities of Mg, Ti and U, which points out that uranium is not associated with analytes containing these major elements. In addition, uranium appears under

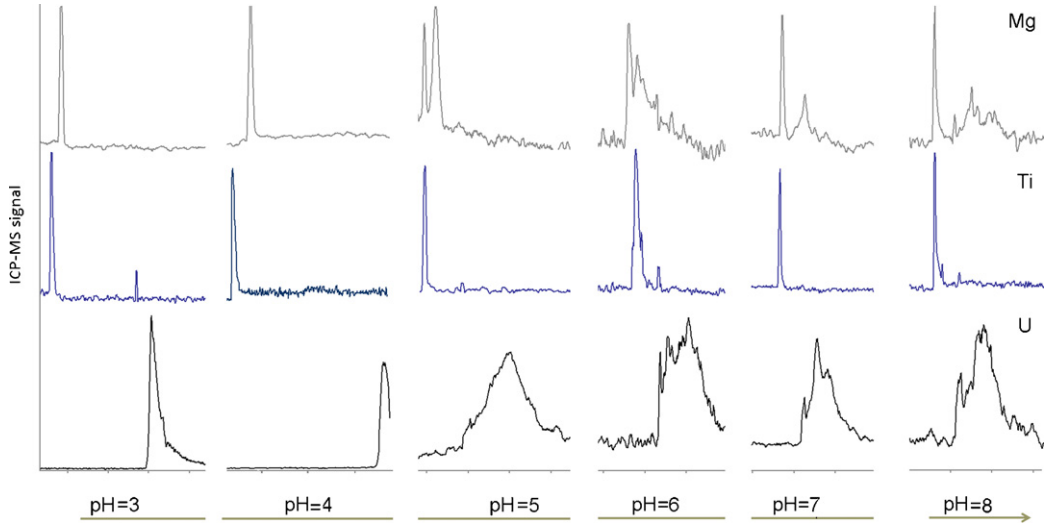

Fig. 4. Uranium, magnesium and titanium electropherograms obtained from the soil leachate at different pH.

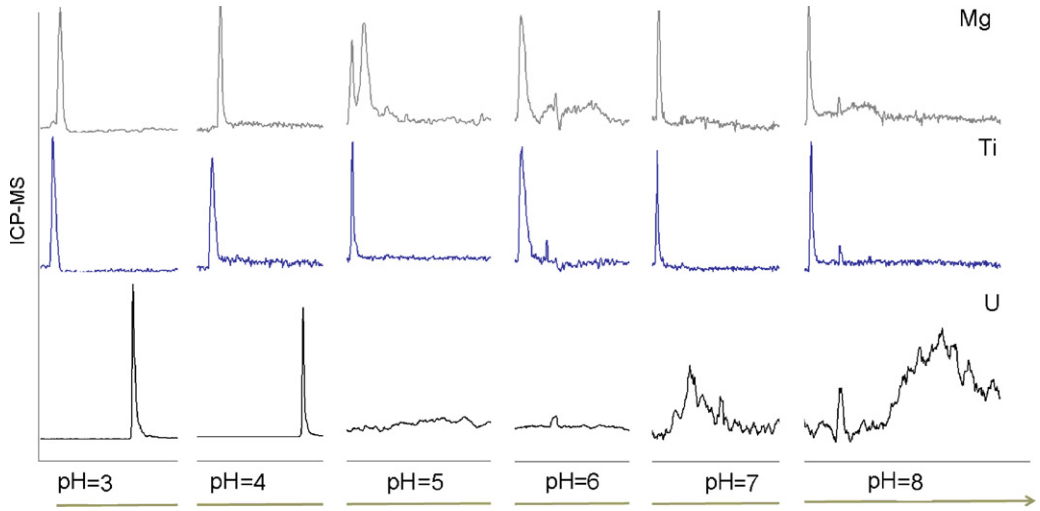

Fig. 5. Uranium, magnesium and titanium electropherograms from the dissolved and colloidal part below 20 nm of the soil leachate at different pH.

dissolved species. The thermodynamic data clearly show the presence of a single dissolved uranium species, UO_2^{2+} (100%); this result is in agreement with the aforementioned experimental data. So, in these conditions, only uranyl species are assumed to be present.

At pH 4, a single uranium peak is again observed (Fig. 4). According to its electrophoretic mobility, uranium and its associated species are anionic. Furthermore, the electrophoretic mobilities of Ti and Mg do not correlate with the uranium one. Besides, according to the thermodynamic data, the present major species expected are UO_2^{2+} (50%) and UO_2CO_3 (50%), the corresponding average charge of dissolved uranium being about 1 (Figs. 2 and 3). The differences observed between the charge experimentally determined and the charge calculated could be explained by the sorption of uranium under cationic or neutral species onto colloids negatively charged, thanks to electrostatic interactions for example. The resulting charge would not be counterbalanced, leading to the detection of anionic species. However, it appears that uranium is mainly present in the compartment < 20 nm. Thus, it is likely that U interacts with small-size colloids lower than 20 nm, according to the experimental conditions. Given the lack of correlation between Mg, Ti and U electrophoretic mobilities and according to the data obtained from the characterization of the colloidal phase, U cannot be sorbed onto the inorganic colloidal fraction previously observed. So uranium would be associated with organic ligands having such a size and a nature that they were not detected by As-Fl-FFF-UV-MALLS. Typically, it could be organic exudates such as polysaccharides or humic/fulvic based substances. This last hypothesis is also strengthened by the value of the pKa of fulvic acids established from 2.8 and 4.6 according to the presence of different carboxylic group types [35]. Furthermore, numerous authors in the literature have already proved that humic substances have great affinities for the uranyl species at environmental pH [36,37].

At pH 5, one broad band is observed for uranium and one or two peaks for major elements (Fig. 4). The electrophoretic mobility allows concluding that uranium appears again under negatively charged species, in the colloidal fraction superior to 20 nm. Main uranium species determined thanks to thermodynamic data are UO_2^{2+} (5%), UO_2OH^+ (2%) and UO_2CO_3 (93%), with an average charge close to zero. The hypothesis of uranium sorption phenomena onto carbon-based colloids is then relevant. It could be inorganic carbon based colloids mainly constituted by carbonated species, or organic ligands with such a size and a nature that they are not detected by As-Fl-FFF-UV-MALLS. According to the lack of calcium in the colloidal carriers observed here, the hypothesis of uranium interactions with organic carbon-based colloids such as polysaccharides or humic-like substances is strengthened.

At pH 6, one peak associated to uranium is located in the anionic region of the electropherogram. Regarding the identification of the uranium species, the speciation calculations show the presence of UO_2CO_3 (15%), $UO_2(CO_3)_2^{2-}$(70%) and $UO_2(CO_3)_3^{4-}$(15%) with an average charge globally negative. Thus, the calculations data are in agreement with the experimental ones, with the appearance of uranium carbonated dissolved species. According to the calculations, when the pH increases, the dissolved uranium cationic species disappear gradually and are replaced by anionic ones. This disappearance also corresponds to the appearance of carbonates. So, from the experimental observations, the presence of carbonates would lead to the progressive desorption of uranium from colloids to the dissolved phase, thanks to the great affinity between uranium and carbonates (see Table 1).

At pH 7 and 8, this hypothesis is strengthened by the observations made on the electropherograms obtained, where uranium reappears gradually as anionic and dissolved forms (at pH 7 approximately 50% of desorption and, at pH 8, a complete desorption

Table 3
Summary of the different results obtained during this study.

pH	Uranium speciation	Uranium location	Comments
3	UO_2^{2+} (100%)	Dissolved	Agreement calculations/experiments
4	UO_2^{2+} (50%), UO_2CO_3 (50%)	Dissolved and colloidal (<20 nm)	Uranium sorption phenomena onto colloids (<20 nm)
5	UO_2^{2+} (5%), UO_2OH^+ (2%), UO_2CO_3 (93%)	Colloidal (20–450 nm)	Uranium sorption phenomena onto colloids (20–450 nm)
6	UO_2CO_3 (15%), $UO_2(CO_3)_2^{2-}$(70%), $UO_2(CO_3)_3^{4-}$ (15%)	Dissolved and colloidal	Gradual desorption of uranium from colloids to the dissolved fraction (carbonates)
7	$UO_2(CO_3)_3^{4-}$ (100%)		
8	$UO_2(CO_3)_3^{4-}$ (100%)		

according to the intensity of peaks on Fig. 5), while the concentration of carbonated species increases (Fig. 2).

All the observations made throughout this study are summarized in Table 3.

4. Conclusions

The uranium–colloid interactions in a specific soil were investigated in this work. In order to characterize the different uranium colloidal carriers, As-Fl-FFF-UV-MALLS-ICP-MS analysis was performed. A size colloidal continuum was identified as aggregates probably constituted of inorganic colloidal Ti, Mg, Ca, Fe, Al-rich and carbon-based particles as well as organic matter. Then, one or two peaks were observed by CE-ICP-MS, for the major elements present in the leaching solutions, depending on pH value. The different mobilities, experimentally determined, which were used jointly to the information from colloidal fraction characterization, allowed concluding first of all that uranium species observed are cationic at pH 3 and anionic from pH 4 to 8. By comparing speciation calculations and CE and As-Fl-FFF experimental data, positive uranium species appear involved in interactions with negatively charged colloids. This process is strongly pH dependent, with a gradual desorption of uranium species from pH 7. Finally, all these results stress that the colloidal species may play a significant role in the uranium distribution in this natural soil, on the surface and sub-surface. The accurate structures of the colloidal species are still unknown but they necessarily contain an organic part. This structure could be investigated in the future by separative techniques coupled with mass spectrometry (ESI-MS or tandem MS). Another possibility could be the use of microscopy techniques (SEM, TEM, AFM) allowing a direct approach in order to obtain a picture of the colloid describing its structure and/or its chemical composition. However, these techniques suffer of poor sensibility and reproducibility.

References

[1] F. Paquet, C. Guillermin, E. Ansoborlo, K. Beaugelin-Seiller, M. Carrière, I. Dublineau, F. Taran, C. Vidaud, L'uranium in toxicologie nucléaire, environnementale et humaine, Lavoisier Ed, Paris, 2009.
[2] IUPAC, Compendium of Chemical Terminology, 2nd ed., Blackwell Scientific, New York, 1997.
[3] A.M. Ure, C.M. Davidson, Chemical Speciation in the Environment, Blackie Academic and Professional, 1995.
[4] K.V. Ticknor, P. Vilks, T.T. Vandergraaf, Appl. Geochem. 11 (1996) 555–565.
[5] V. Moulin, C. Moulin, Appl. Geochem. 10 (1995) 573–580;
N. Banik, L. Buda, S. Bürger, J.V. Kratz, N. Trautmann, J. Alloys Comp. 444–445 (2007) 522–525.
[6] I.A.M. Worms, Z. Al-Gorani Szigeti, et al., Water Res. 44 (2010) 340–350.
[7] A.J. Bednar, V.F. Medina, D.S. Ulmer-Scholle, B.A. Frey, B.L. Johnson, W.N. Brostoff, S.L. Larson, Chemosphere 70 (2007) 237–247.
[8] J. Mibus, S. Sachs, W. Pfingsten, C. Nebelung, G. Bernhard, J. Contam. Hydrol. 89 (2007) 199–217.
[9] J.F. Ranville, M.J. Hendry, T.N. Reszat, Q. Xie, B.D. Honeyman, J. Contam. Hydrol. 91 (2007) 233–246.
[10] B.P. Jackson, J.F. Ranville, P.M. Bertsch, A.G. Sowder, Environ. Sci. Technol. 39 (2005) 2478–2485.
[11] M. Matsunaga, S. Nagao, T. Ueno, S. Takeda, H. Amano, Y. Tkachenko, Appl. Geochem. 19 (2004) 1581–1599.
[12] R. Artinger, T. Rabung, J.I. Kim, S. Sachs, K. Schmeide, K.H. Heise, G. Bernhard, H. Nitsche, J. Contam. Hydrol. 58 (2002) 1–12.
[13] A.B. Kersting, D.W. Efurd, D.L. Finnegan, D.J. Rokop, D.K. Smith, J.L. Thompson, Nature 39717 (1999) 56–59.
[14] S. Utsunomiya, A.B. Kersting, R.C. Ewing, Environ. Sci. Technol. 43 (2009) 1293–1298.
[15] E. Bolea, M.P. Gorriz, M. Bouby, F. Laborda, J.R. Castillo, H. Geckeis, J. Chromatogr. A 1129 (2006) 236–246.
[16] G.A. Braun, U. Lankes, F.H. Frimmel, Aqua. Sci. 66 (2004) 151–170.
[17] S. McDonald, A.G. Bishop, P.D. Prenzler, K. Robards, Anal. Chim. Acta 527 (2004) 105–124.
[18] H. Geckeis, T.N. Manh, M. Bouby, J.I. Kim, Colloids Surf. A 217 (2003) 101–108.
[19] P. Janos, J. Chromatogr. A 983 (2003) 1–18.
[20] L.J. Gimbert, K.N. Andrew, P.M. Haygarth, P.J. Worsflod, Trends Anal. Chem. 22 (10) (2003) 615–633.
[21] E. Alasonati, S. Dubascoux, G. Lespes, V.I. Slaveykova, Environ. Chem. 44 (2010) 215–223.
[22] N. Surugau, P.L. Urban, J. Sep. Sci. 32 (2009) 1889–1906.
[23] M. Potin-Gautier, C. Casiot, F. Pannier, Spectra Anal. 221 (2001) 23–30.
[24] S. Pompe, K.H. Heise, H. Nitsche, J. Chromatogr. A 723 (1996) 215–218.
[25] P.K. Egeberg, S.O. Bergli, J. Chromatogr. A 950 (2002) 221–231.
[26] H.W. Sun, P. He, Y.K. Lu, S.X. Liang, J. Chromatogr. B 852 (2007) 145–151.
[27] C. Ambard, Ph.D. Thesis, Université de Paris XI – UFR scientifique d'Orsay, 2006.
[28] M. Hosse, K.J. Wilkinson, Environ. Sci. Technol. 35 (2001) 4301–4306.
[29] J.W. Olesik, J.A. Kinzer, E.J. Grunwald, K.K. Thaxton, S.V. Olesik, Spectrochim. Act. Part B 53 (1998) 239–251.
[30] AFNOR, norme AFNOR X31-210 Déchets, essais de lixiviation, normalisation française, 1992.
[31] C.M. Davies, C.M. Ferguson, C. Kaucner, M. Krogh, N. Altavilla, A.D. Deere, N. Ashbolt, Appl. Environ. Microbiol. 70 (2004) 1151–1159.
[32] C. Claveranne-Lamolere, G. Lespes, J. Aupiais, F. Pointurier, M. Potin-Gautier, J. Chromatogr. A 1216 (2009) 9113–9119.
[33] M.E. Schimpf, K.D. Caldwell, J.C. Giddings, Field-Flow Fractionation Handbook, Wiley Interscience, New York, 2000.
[34] S. Topin, J. Aupiais, P. Moisy, Electrophoresis 30 (2009) 1747–1755.
[35] A.A.A.C. Machado, J.C.G. Esteves Da Silva, Chem. Intel. Lab. Syst. 17 (1992) 249–258.
[36] K.R. Czerwinski, G. Buckau, F. Scherbaum, J.I. Kim, Radiochim. Acta 65 (1994) 111–119.
[37] J.J. Lenhart, S.E. Cabaniss, P. McCarthy, B.D. Honeyman, Radiochim. Acta 88 (2000) 345–353.